Transfer of Long-Chain Fluorescent Fatty Acids between Small and Large Unilamellar Vesicles†

Alan M. Kleinfeld*,‡ and Judith Storch§,‖

Division of Membrane Biology, Medical Biology Institute, La Jolla, California 92037, and Department of Nutrition, Harvard School of Public Health, 665 Huntington Avenue, Boston, Massachusetts 02115

Received September 3, 1992; Revised Manuscript Received December 11, 1992

ABSTRACT: Transfer of 12-(9-anthroyloxy)stearic acid (12AS) was measured between small unilamellar vesicles (SUV) and between large unilamellar vesicles (LUV), over a temperature range of 5–50 °C. The results of this study clearly establish the biexponential nature of the time dependence of the transfer in a variety of vesicle types and confirm our previous results using egg phosphatidylcholine (EPC) SUV at 25 °C (Storch & Kleinfeld, 1986). In our previous study we developed a kinetic model of the transfer process and concluded that the observed time dependence of the transfer of long-chain 12-(9-anthroyloxy) fatty acids (AOFA) was due to transbilayer flip-flop that was much slower than the rate at which the fatty acids (FA) move from the vesicle and into the surrounding aqueous phase (the off step). In the present study, experimental and theoretical advances have allowed us to examine, in detail, predictions of the kinetic model that critically depend upon the slow rate of flip-flop. The current results verify these predictions and demonstrate that slow AOFA flip-flop is rate limiting in at least three different vesicle systems and at all temperatures studied. Moreover, both flip-flop and the off rate constants were almost an order of magnitude smaller in EPC-LUV than in EPC-SUV. Flip-flop was found to be asymmetric (the rate constant for transfer from the inner to outer hemileaflet of the bilayer is approximately twice that from the outer to inner hemileaflet) in SUV but virtually symmetric in LUV. The temperature dependence of transfer was used to determine the thermodynamic activation potentials for the flip-flop and off rate constants. The barriers for these steps were sensitive functions of vesicle size, lipid composition, and bilayer physical state. In particular, while enthalpic contributions dominate both the flip-flop and off steps in liquid crystalline SUV, entropic factors dominate the activation barriers in LUV and in gel-state SUV. Thus, the hydrophobic AOFA molecules transfer across the lipid bilayer slowly, and the interactions which govern their movement both across and between lipid vesicles are a complex function of the composition and structure of the bilayer.

Long-chain fatty acids (FA)[1,2] are essential to many important physiological processes. Utilization of FA in these processes requires that FA be transported across cell membranes. Cellular transport studies have resulted in two, quite divergent views of the mechanism of transmembrane movement (flip-flop). In the first, it is thought that FA transport occurs through rapid movement across the lipid bilayer phase of the membrane by simple diffusion (DeGrella & Light, 1980; Daniels et al., 1985; Noy et al., 1986; Cooper et al., 1989). The second view is that for the physiologically important long-chain FA, transport is directly mediated by a membrane transport protein (Shohet et al., 1968; Nunn et al., 1979; Paris, et al., 1979; Abumrad et al., 1984; Morand & Aigrot, 1985; Potter et al., 1989). These two views make contradictory predictions for the rate of FA flip-flop in lipid bilayers (Storch, 1990). The first mechanism predicts, as expected from the conventional view that lipid permeability increases with increasing hydrophobicity, that the rate of transbilayer flip-flop of long-chain FA is not rate-limiting. In contrast, the second mechanism predicts that the FA flip-flop rate is slower than the rate required for cellular FA transport.

Our own studies as well as others have demonstrated that FFA can spontaneously transfer between and through the bilayer of pure lipid vesicles (Doody et al., 1980; Storch & Kleinfeld, 1986; Gutknecht, 1988). *Short-chain* FA (≤C12) appear to undergo extremely rapid transbilayer flip-flop and it is likely that the off step (movement of the FFA from the bilayer into the aqueous phase) is rate-limiting for this process (Doody et al., 1980; Hamilton, 1989). There is, however, considerable disagreement as to the rate and mechanism of *long-chain* FA transfer. Transfer of long-chain natural FA between small unilamellar vesicles (SUV) and albumin has been used to suggest that the off step from SUV is rate-limiting and that the rate of flip-flop is extremely fast, $>4\ s^{-1}$ (Daniels et al., 1985). On the other hand, studies of oleate transfer into or out of multilamellar vesicles (MLV) suggest that flip-flop, at least in these vesicles, is relatively slow, perhaps $<0.0008\ s^{-1}$ (Kleinfeld, 1990). In addition, a very slow flip-flop rate of $<10^{-4}\ s^{-1}$ was found in planar bilayers for the anionic form of the FA (Gutknecht, 1988). Previous studies have demonstrated that the rate of FA transfer increases with pH, suggesting that the anionic form is not rate-limiting (Doody et al., 1980; Storch & Kleinfeld, 1986) and therefore that the flip-flop rate constant of $10^{-4}\ s^{-1}$ found in planar bilayers represents an upper limit. The large differences in flip-flop rates inferred from these studies indicate the difficulty in determining the flip-flop mechanism of natural FA

† This work was supported by grants from the NIH (GM44171 to A.M.K. and DK38389 to J.S.).

‡ Medical Biology Institute.

§ Harvard School of Public Health.

‖ Present address: Department of Nutritional Sciences, Rutgers University, New Brunswick, NJ 08903.

[1] Abbreviations: AOFA, *n*-(9-anthroyloxy) fatty acid; 12AS, 12-(9-anthroyloxy)stearic acid; DMPC, dimyristoylphosphatidylcholine; EPC, egg phosphatidylcholine; FA, fatty acid(s); FFA, free fatty acid(s); LUV, large unilamellar vesicle(s); MLV, multilamellar vesicle(s); PC, phosphatidylcholine; SUV, small unilamellar vesicle(s).

[2] The term fatty acid (FA) as used here refers to the acid, salt, or ionized molecule, whether membrane-bound or free. Free fatty acid (FFA) refers to the aqueous-phase monomer of the molecule.

0006-2960/93/0432-2053$04.00/0

(Kleinfeld, 1990). Since similar constraints on the movement of natural FA probably apply to fluorescent FA analogs, we previously investigated the transfer of the *n*-(9-anthroyloxy) FA (AOFA) between egg phosphatidylcholine (EPC) SUV (Storch & Kleinfeld, 1986). The fluorescent properties of the AOFA allow a detailed determination of the vesicle transfer kinetics. We found that the kinetics of long-chain AOFA transfer were biexponential, and this indicated that transfer of long-chain AOFA involved a slow flip-flop step followed by a much faster off rate from the membrane.

In order to explore further this mechanism of long-chain AOFA movement and to begin to define the molecular bases of the barriers to the flip-flop and off steps, we have extended our previous studies, which were done at a single temperature (25 °C) using EPC-SUV (Storch & Kleinfeld, 1986). We have now examined 12-(9-anthroyloxy)stearate (12AS) transfer between EPC-SUV, between DMPC-SUV, and between EPC large unilamellar vesicles (LUV) over a temperature range of 5–50 °C. The improved quality of the data and the much slower transfer rates obtained with LUV and DMPC-SUV have allowed a more rigorous testing of our previously described kinetic model (Storch & Kleinfeld, 1986). Together with extensions of the kinetic theory for this model, the present data demonstrate that slow AOFA flip-flop is a general property of transbilayer movement and that the barriers to the various steps in intervesicle transfer are extremely sensitive to donor vesicle structure and composition.

MATERIALS AND METHODS

Materials. Egg phosphatidylcholine (EPC), *N*-(7-nitro-2,1,3-benzoxadiazol-4-yl)phosphatidylethanolamine (NBD-PE), and dimyristoylphosphatidylcholine (DMPC) were purchased from Avanti Polar Lipids (Birmingham, AL). 12-(9-Anthroyloxy)stearic acid was purchased from Molecular Probes (Eugene, OR). The standard buffer was 20 mM Tris and 50 mM NaCl at pH 7.6.

Vesicle Preparation. SUV were prepared essentially by the method of Huang and Thompson (1974), as described previously (Storch & Kleinfeld, 1986), and LUV were prepared essentially by the method of Nozaki et al. (1982) also as described previously (Cardoza et al., 1984). Either unlabeled lipid alone (donor vesicles) or unlabeled lipid plus 10 mol % NBD-PE (acceptor vesicles) was dried overnight, under vacuum, to remove organic solvent. For SUV the dried lipid film was hydrated by addition of buffer, the dispersion was sonicated at 70 W for 30 min, and the sonicated dispersion was centrifuged at 105000*g* for 45 min to remove titanium and lipid debris. Vesicles prepared from EPC were maintained at all times during preparation at ~4 °C, while DMPC vesicles were maintained at about 30 °C. For LUV the dried lipid film was dissolved in 100 mM *n*-octyl β-glucopyranoside and the mixture (~5 mL) was dialyzed against 2 L of standard buffer and the dialysate was changed each day for 3 days. Thin-layer chromatography in chloroform/methanol/acetic acid/water (25:15:4:2) was done to assess integrity of vesicle lipid. No degradation of lipid was observed as a consequence of vesicle preparation or time of incubation. Several samples of NBD-PE, however, exhibited, in addition to the primary NBD-PE peak, polar components that did not migrate from the origin. These samples were not used in these studies since acceptor vesicles prepared with this material displayed an additional, very fast, component of quenching.

Transfer Assay. Transfer of AOFA from donor to acceptor vesicles was determined from the time-dependent decrease in AOFA fluorescence that occurs after mixing donor and acceptor vesicles. This decrease in fluorescence occurs because AOFA moves from the donor vesicle, where it is highly fluorescent, to the aqueous phase and then to the NBD-PE-labeled acceptor vesicle. In both these locations AOFA fluorescence is quenched to greater than 97%. Donor vesicles in equilibrium with 12AS were produced by adding 12AS to vesicle suspensions from stock solutions in ethanol so that the final ethanol concentration was <0.1% by volume. Typically, the lipid concentration of the donor vesicles was 50 μM, acceptor vesicles 100–500 μM, and 12AS about 1 μM. In our previous study of long-chain AOFA transfer between SUV composed of EPC, the decay of donor 12AS fluorescence was determined at about 20 discrete times following rapid vortex mixing of donor and acceptor vesicles (Storch & Kleinfeld, 1986). In the present study a Hi-Tech (SFA-11) stopped-flow device with a dead time of about 20 ms was used to mix donor and acceptor vesicles. The stopped-flow device was interfaced with an SLM 8000C fluorometer which allowed the accumulation of approximately 1000 intensities, by photon counting, per transfer scan. Transfer measurements were carried out for times $\leq 3/k_1$, where k_1 is the decay constant for a single-exponential fit to the intensities, because this time range was found to correctly return decay parameters in fits to biexponential intensities simulated with Gaussian noise (data not shown). Fluorescence intensities were determined with an excitation wavelength of 383 nm, excitation slits of 1 nm, emission wavelength of 455 nm, and emission slits of 16 nm. Under these conditions and for scan times $\sim 3/k_1$, photobleaching of 12AS was less than 0.5%/min and did not significantly affect the analysis.

Data Analysis. A minimum of three scans were accumulated for each experimental condition and each scan was fitted to both single- and double-exponential functions:

$$F(t) = \alpha e^{-kt} + C \quad (1)$$

$$F(t) = \alpha_f e^{-k_f t} + \alpha_s e^{-k_s t} + C \quad (2)$$

where $\alpha + C = 1$ and $\alpha_f + \alpha_s + C = 1$, as described previously (Storch & Kleinfeld, 1986; Kleinfeld, 1990). Fit quality was assessed by fit residuals and by the value of χ^2 normalized to the number of degrees of freedom (~1000). Fit residuals were evaluated as $[F(t) - I(t)]/\sigma$, where $F(t)$ is either eq 1 or 2 and $I(t)$ is the measured fluorescent intensity determined by photon counting (number of photons at time t). For each intensity, $I(t)$, the standard deviation (σ) was taken as $[I(t)]^{1/2}$. In virtually all the measurements χ^2 values were distributed about 1.0 (acceptable) for the two-exponential fits, while χ^2 values were virtually all >1.5 ($p < 0.05$) (unacceptable) for fits with eq 1.

Kinetic Model. We have previously described a kinetic model for transfer of FA between identical lipid bilayer vesicles (Storch & Kleinfeld, 1986; Kleinfeld, 1990). In this model $C_i(t)$ represents the time-dependent concentrations of AOFA in the inner and outer hemileaflets of the donor ($i = 1, 2$) and acceptor ($i = 5, 4$) bilayers and the aqueous phase separating the vesicles ($i = 3$). The intrinsic rate constants for transfer from inner to outer hemileaflet, from outer to inner hemileaflet, from outer hemileaflet into the aqueous phase, and from the aqueous phase onto the outer hemileaflet are, respectively, k_{12}, k_{21}, k_{off}, and k_{on}. As described previously (Storch & Kleinfeld, 1986), the differential equations that determine the $C_i(t)$ are

$$dC_1(t)/dt = k_{21}C_2(t) - k_{12}C_1(t) \quad (3)$$

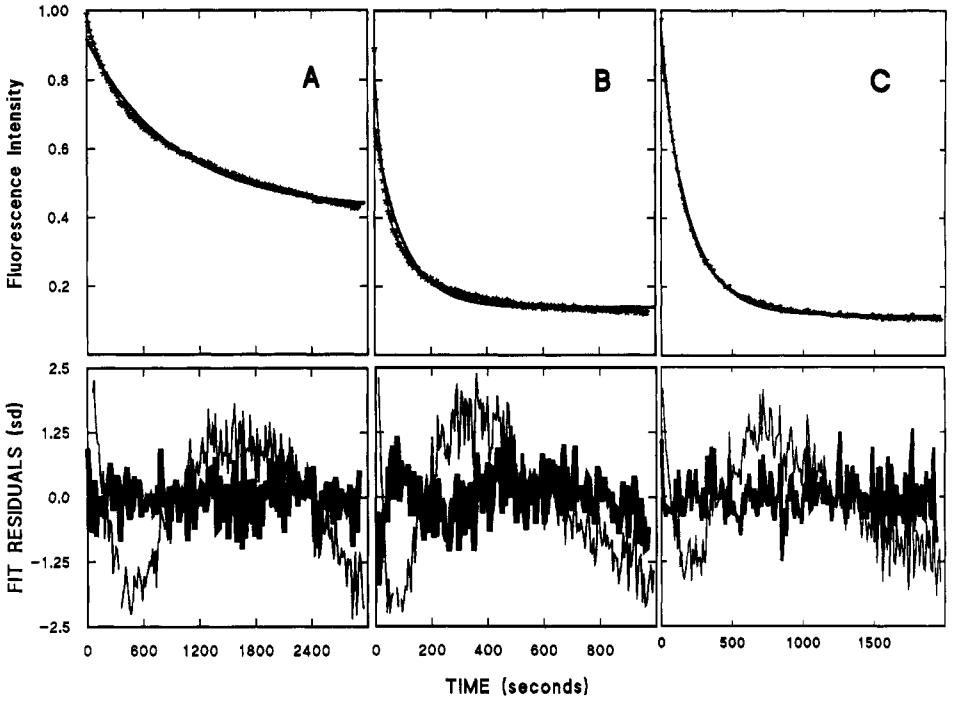

FIGURE 1: Kinetics of 12AS transfer between donor vesicles at 30 °C. The upper panels show the fluorescence of 12AS as a function of time after stopped-flow mixing of donor vesicles with an excess of acceptor vesicles. (A) EPC-LUV; (B) EPC-SUV; (C) DMPC-SUV. As discussed in the text, the fluorescence intensity is directly proportional to the concentration of 12AS remaining in the donor vesicles. Depending upon vesicle type and temperature, the fluorescence intensity (here normalized to the intensity at time zero) decays at varying rates to a constant value that at equilibrium ($t = \infty$) is directly proportional to the ratio of donor to total (donor + acceptor) vesicle concentration. In these measurements donor vesicles were preincubated for times > 7 half-times of the decay before being mixed with acceptor vesicles. As discussed in the text, the average of five neighboring measured intensities is plotted as an open star. The optimal single- (eq 1) and double- (eq 2) exponential fits to each decay are shown, respectively, as solid heavy and light curves through the data. The parameters of these fits are shown in Table I. In the corresponding bottom panels the fit residuals for both the single- (light lines) and double- (heavy lines) exponential fits are plotted in units of the standard deviation of each intensity. In all cases the residuals of the single-exponential fits exceed the vertical scale limits, generally by a factor of 2–4, at early times. Vesicle and 12AS concentrations used in these measurements were approximately as follows: for both EPC and DMPC-SUV, [donor lipid] = 25 μM, [acceptor lipid] = 250 μM, and [12AS] = 0.5 μM; for EPC-LUV, [donor lipid] = 25 μM, [acceptor lipid] = 75 μM, and [12AS] = 0.5 μM.

$$dC_2(t)/dt = k_{12}C_1(t) + k_{on}[D]C_3(t) - k_{21}C_2(t) - k_{off}C_2(t) \quad (4)$$

$$dC_3(t)/dt = k_{off}[C_2(t) + C_4(t)] - k_{on}[T]C_3(t) \quad (5)$$

$$dC_4(t)/dt = k_{12}C_5(t) + k_{on}[A]C_3(t) - k_{21}C_4(t) - k_{off}C_4(t) \quad (6)$$

$$dC_5(t)/dt = k_{21}C_4(t) - k_{12}C_5(t) \quad (7)$$

in which [T] = [D] + [A] and [D] and [A] are the concentrations of the donor and acceptor vesicles, respectively.

In our first study using this model we showed that the observed kinetic parameters could be related to the intrinsic rate constants by closed algebraic expressions (Storch & Kleinfeld, 1986). More recently we have developed an algorithm that allows the three intrinsic rate constants k_{12}, k_{21}, and k_{off} to be determined uniquely from the observed kinetic parameters (Kleinfeld, 1990). This algorithm uses equations A11 and A12 of Storch and Kleinfeld (1986) to express k_{21} (the rate constant for transfer from outer to inner donor bilayer hemileaflet) and k_{off} in terms of k_{12} (the rate constant for inner to outer hemileaflet transfer) and the observed rate constants (k_s and k_f) as follows:

$$k_{21} = [-(k_s - k_f)(k_f k_s) - k_{12}[(k_s)^2 - (k_f)^2] - (k_{12})^2(k_s - k_f)]/[k_{12}(k_s - k_f)] \quad (8)$$

$$k_{off} = -[(k_f)^2 + k_f(k_{12} + k_{21})]/(k_f + k_{12}) \quad (9)$$

Using these equations, expressions for the amplitudes predicted by the model of Storch and Kleinfeld (1986), equations A11, A12, A14, and A15 in the appendix of Storch and Kleinfeld (1986), are reduced to functions of the single variable k_{12}. The value for k_{12} can then be solved numerically using the experimentally determined amplitudes.

RESULTS

Kinetics of 12AS Transfer between Lipid Vesicles Is Biexponential. Typical time courses of donor vesicle-associated 12AS fluorescence at 30 °C, following rapid mixing with excess acceptor vesicles, are shown in Figure 1. The figure shows the decay of 12AS fluorescence intensity and the one- and two-exponential fits to data for EPC-LUV, EPC-SUV, and DMPC-SUV. In each decay, intensities at approximately 1000 time points were accumulated. Since it is difficult to visually identify some of the features of these decays when all ~1000 time points are plotted, we have, in these figures, plotted the average of five neighboring intensities as a star. Nonlinear fits to each decay were done using eqs 1 and 2 to the full data set of ~1000 intensities, and the results are shown as the dark and light solid lines, respectively, in the upper panels of Figure 1. The corresponding fit parameters are listed in Table I. Inspection of these figures reveals that the single-exponential fit fails to describe the decay of the fluorescence intensities. This is clearly apparent in the corresponding lower panels, where the fit residuals are plotted in units of the standard deviation of the observed intensities. As these residuals show, the single-exponential

Table I: Observed Fit Parameters for the 30 °C 12AS Transfer Data of Figure 1[a]

vesicle	no. of exponentials	α_s	k_s (s^{-1})	α_f	k_f (s^{-1})	C	χ^2
DMPC-SUV	1	0.87	0.0049			0.13	1.90
DMPC-SUV	2	0.23	0.0024	0.66	0.0075	0.11	0.97
EPC-SUV	1	0.79	0.0970			0.21	3.40
EPC-SUV	2	0.31	0.0052	0.54	0.0330	0.15	1.10
EPC-LUV	1	0.54	0.0011			0.46	3.30
EPC-LUV	2	0.43	0.0006	0.21	0.0042	0.36	0.97

[a] Decays shown in the upper panels of Figure 1 were fit with eq 1 or 2. The parameters shown in this table are results averaged from 3 decays. Uncertainties in the fit parameters for each fit were determined from the nonlinear least-squares error matrix. The average of these uncertainties, estimated from the analysis of multiple decays, is approximately 20%. The equilibrium constant, C, correctly reflects the ratio of donor to acceptor vesicle concentrations, which in these measurements was about 1:10 for DMPC-SUV and EPC-SUV and about 1:3 for EPC-LUV.

fit exhibits large and nonuniform excursions from the zero value, whereas residuals of the two-exponential fits are, on average, considerably smaller than one standard deviation and are uniformly distributed about zero. This behavior was exhibited in the more than 200 kinetic traces analyzed for these three vesicle systems. The quality of fit was also evaluated by χ^2 values. In virtually every case these values exceeded 1.5 ($p < 0.05$) for the single-exponential fit, while double-exponential fits had χ^2 values ~ 1.0 ($p \sim 0.5$).

Effects of Vesicle Loading Time Demonstrate Slow Flip-Flop. The above results clearly confirm the requirement for two exponentials in the description of the AOFA transfer kinetics. We have previously suggested that the origin of this behavior is slow transmembrane flip-flop followed by a much faster off rate (Storch & Kleinfeld, 1986). To test that flip-flop is indeed slow (the critical prediction of this model), measurements of AOFA transfer kinetics were carried out as a function of vesicle loading time. These studies were done by measuring transfer from donor vesicles that were incubated with exogenously added 12AS for specific times before transfer was initiated by rapid mixing with acceptor vesicles. Incubation times were chosen to be less than or much greater than the overall transfer time. If flip-flop is slow, then 12AS will preferentially populate the outer leaflet in short time loaded vesicles, but will approach a uniform distribution in both hemileaflets in long time loaded vesicles. This distribution difference should be apparent from the parameters of the transfer curve, since the amplitude of the fast component would be greater in the short time loaded vesicles, but the rate constants should not change. If, on the other hand, flip-flop were rapid as compared to the off rate, then time of incubation should not affect the transfer kinetics.

In our previous study with EPC-SUV, overall transfer times (~ 1 min) were quite short compared to the shortest time of preincubation that was technically practical, and therefore the effects of short time loading were only marginally detectable (Storch & Kleinfeld, 1986). As Figures 1 and 2 show, AOFA transfer from EPC-LUV is approximately an order of magnitude slower than that from EPC-SUV. Thus, if both off rate and flip-flop are reduced proportionately in LUV compared to SUV, the effects of differential loading time would be much more apparent in LUV than SUV. As the data in Figure 2 demonstrate, this is indeed the case. In the upper two decays, LUV were incubated with 12AS for either more than 2 h or less than 5 min. The shapes of these two curves show that the amplitude of the rapidly transferring component is considerably greater from donor vesicles incubated with 12AS < 5 min as compared to a >2-h incubation.

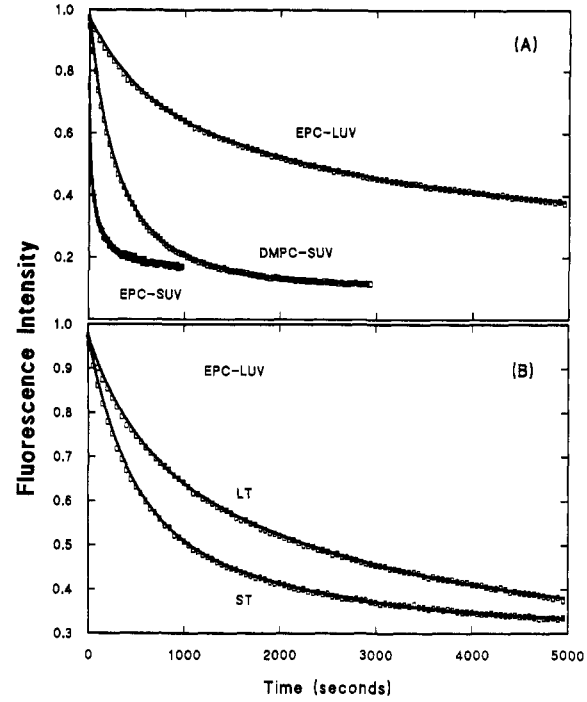

FIGURE 2: Effects on transfer kinetics of 12AS loading time, vesicle structure, and vesicle composition. The fluorescence intensity of 12AS was measured at 25 °C (or 24 °C in the case of DMPC) by the same methods and conditions as described in the caption to Figure 1. In this figure the average of 10 measured intensities was plotted as an open box. The solid curves represent the best two-exponential fit to the data and the corresponding fit parameters are given in Table II. (A) Transfer from long time loaded ($>10k_1$) EPC-SUV, DMPC-SUV, and EPC-LUV. (B) EPC-LUV preincubated with 12AS for either 2 h (LT) or 5 min (ST) before stopped-flow mixing with acceptor vesicles.

Table II: Observed Fit Parameters for the 25 °C 12AS Transfer Data of Figure 2[a]

vesicle	no. of exponentials	α_s	k_s (s^{-1})	α_f	k_f (s^{-1})	C	χ^2
LUV-ST	1	0.62	0.0012			0.38	5.30
LUV-ST	2	0.29	0.0005	0.39	0.0022	0.32	0.87
LUV-LT	1	0.60	0.0007			0.40	4.50
LUV-LT	2	0.45	0.0004	0.23	0.0025	0.32	0.90
DMPC-SUV	1	0.86	0.0023			0.14	5.00
DMPC-SUV	2	0.36	0.0013	0.53	0.0043	0.11	0.92
EPC-SUV	1	0.77	0.0770			0.23	2.10
EPC-SUV	2	0.31	0.0047	0.47	0.0420	0.22	0.89

[a] Methods are as described in the legend to Table I. Measurements done with LUV designated with ST or LT indicate short time (<5 min) or long time (>2 h) incubation of donor LUV with 12AS, respectively.

The observed kinetic parameters for these two curves, shown in Table II, indicate that the shape differences are due entirely to the differences in amplitudes since the observed rate constants are virutally unchanged. In particular, the ratio of fast to slow amplitudes, α_f/α_s, increases from 0.5 for long time incubation to 1.3 for short time incubation, a 260% change that is significant since the amplitude uncertainties are $\sim 20\%$. Additional processes that might contribute to the biexponential character of the decay are those due to vesicle collision or effects of AOFA clustering within the donor vesicle. Although neither of these were found to be significant in our previous study of 12AS transfer between SUV (Storch & Kleinfeld, 1986), because the slower transfer times increase the possibility that vesicle collision might contribute to AOFA transfer in LUV, we also carried out transfer measurements in LUV as a function of acceptor and 12AS concentrations. Varying

Table III: Intrinsic Rate Constants for 12AS Transfer at 25 °C[a]

vesicle	k_{12} (s^{-1})	k_{21} (s^{-1})	k_{off} (s^{-1})
EPC-LUV	0.00057	0.00054	0.0022
EPC-SUV	0.00500	0.00230	0.0390
DMPC-SUV	0.00100	0.00037	0.0033

[a] Methods are as described in the legend to Table I. Intrinsic rate constants were determined from the observed kinetic parameters given in Table II using the algorithm described in Materials and Methods. LUV values are those for long time (>2 h) loading.

acceptor and 12AS concentrations approximately 10–fold had no effect on k_i or α_i values (data not shown).

Large Differences between k_s and k_f Indicate That Flip-Flop Is Slower Than the Off Rate. Intrinsic rate constants were determined from the observed kinetic parameters for the data of Figure 2 using the solutions to eqs 3–7 as described in Materials and Methods. These results are shown in Table III, where it is seen that AOFA flip-flop and off rate constants are approximately equal to k_s and k_f, respectively. This near equality is predicted by the model to occur only when the flip-flop and off rate constants differ by more than about 5–10-fold (Kleinfeld, 1990). Thus for all three vesicles systems the flip-flop rate constants are much less than the off rate. This result is contrary to the view that very hydrophobic molecules display rapid flip-flop in comparison to the off rate (Doody et al., 1980; Daniels et al., 1985).

Transfer Parameters Are Sensitive to Vesicle Radius of Curvature and Composition. As seen in Figures 1 and 2 and in Tables I and II, transfer of 12AS is much slower from EPC-LUV than from EPC-SUV, and both k_f and k_s are reduced. Since flip-flop and off rates can be resolved, these results demonstrate that increasing the radius of curvature decreases the flip-flop rate as well as the off rate (see Figure 4). A comparison of EPC-SUV with results for DMPC-SUV, which are also shown in Figures 1 and 2 and Tables I and II, indicate that lipid composition as well as vesicle size plays a significant role in the determination of the kinetic parameters. The results in Figure 1 were obtained at 30 °C, where all three vesicle systems are in the liquid crystalline phase. The significantly greater rates in EPC-SUV as compared to DMPC-SUV therefore reflect a difference in donor phospholipid acyl chain composition.

Flip-Flop Rate Constants Are Symmetric in LUV but Asymmetric in SUV. Another feature of the results in Table III provides important support for the model. The rate constant for transfer from the inner to outer hemileaflet (k_{12}) is twice the reverse rate (k_{21}) in SUV ($k_{12} \sim 2k_{21}$), whereas for LUV these rates are nearly equal ($k_{12} \sim k_{21}$). These results are predicted if, at equilibrium, the FA concentration is equal in both hemileaflets of these vesicles. Since the outer hemileaflet area is about twice that of the inner area in SUV, and these areas are approximately equal in LUV, equal concentrations at equilibrium requires $k_{12} \sim 2k_{21}$ and $k_{12} \sim k_{21}$ in SUV and LUV, respectively.

Temperature Dependence of Transfer Kinetics and the Intrinsic Rate Constants. The results presented above provide strong confirmation of the kinetic model used to describe FA transfer between lipid bilayer vesicles. The solution to this model allows the determination of the intrinsic rate constants from the observed kinetic parameters.[3] These intrinsic rate constants reflect the molecular factors that determine the kinetic barriers to FA movement. To begin to understand these molecular factors we have measured the transfer of 12AS in each of the three vesicle systems as a function of temperature, and the observed kinetic parameters are plotted in Figure 3. The results show that there is substantial admixing of fast and slow components in all three vesicle systems; α_f/α_s ranges between ~0.3 and ~4.0. With the exception of DMPC at temperatures below 24 °C, the observed rate constants increase monotonically throughout the temperature range. For DMPC-SUV the observed amplitudes (α_i) exhibit a substantial alteration at around 24 °C, and rate constants are virtually independent of temperature below 24 °C.

Intrinsic rate constants determined from the observed kinetic parameters of Figure 3 are shown in Figure 4. Solid lines through the data are linear fits throughout the entire temperature range for EPC vesicles, while for DMPC separate fits are shown above and below 24 °C. In these Arrhenius plots, linear behavior is exhibited by both sizes of EPC vesicles, whereas a discontinuity occurs at approximately 24 °C for DMPC. It is also apparent from Figure 4 that both flip-flop rate constants are approximately equal for LUV but differ appreciably for both SUV vesicle types. The slopes and intercepts of these lines were analyzed using Eyring rate theory (Eisenberg & Crothers, 1979) to determine activation potentials for each of the processes represented by these intrinsic rate constants. The results shown in Table IV indicate rather remarkable differences among the various vesicle systems, suggesting quite different barriers to AOFA movement. For vesicles in the liquid crystalline state there are major differences between SUV and LUV. For LUV, the barriers for all steps and especially for flip-flop are dominated by entropic factors, whereas the opposite is generally true for SUV. Below 24 °C the barriers for DMPC have virtually no enthalpic component.

DISCUSSION

Flip-Flop of Long-Chain AOFA Is an Extremely Slow Process in LUV. The results of this study extend our previous findings and show that long-chain AOFA flip-flop is slower than the off step in LUV as well as SUV. The quality of data makes it possible to establish the biexponential nature of the transfer kinetics with virtual certainty and, as a consequence, to examine predictions of the kinetic model in detail. An important prediction of the model, which follows directly from a slow AOFA flip-flop followed by a much faster off step, is that decreasing AOFA loading time increases the proportion of the fast component of the observed transfer kinetics. The results in LUV (Figure 2 and Table II) clearly verify this prediction. Moreover, by extending the kinetic model to allow both flip-flop rate constants to be determined from the observed kinetic parameters, we showed directly that flip-flop is asymmetric in SUV and virtually symmetric in LUV, thereby lending further support to the model. Thus, the transfer of AOFA between bilayer vesicles proceeds by slow flip-flop followed by a much faster off step, and both these steps are substantially slower in LUV than in SUV (Table III).

Trends similar to the decrease in 12AS vesicle transfer rates with vesicle size have also been observed using other lipophiles. Five-fold slower cholesterol transfer rates were observed in EPC/cholesterol LUV as compared to SUV (McLean & Phillips, 1984a). Cholesterol transfer kinetics were single-exponential, suggesting that the increase in radius of curvature principally affected the off rate. Similar effects of vesicle size, although of smaller magnitude (a 2-fold difference), were observed for the off rate of DMPC from DMPC vesicles

[3] Since the initial conditions for this solution require a steady-state distribution of FA among the inner and outer hemileaflets of the bilayer and the aqueous phase at time zero (Storch & Kleinfeld, 1986), this solution cannot be used to determine the intrinsic rate constants for short time loading conditions.

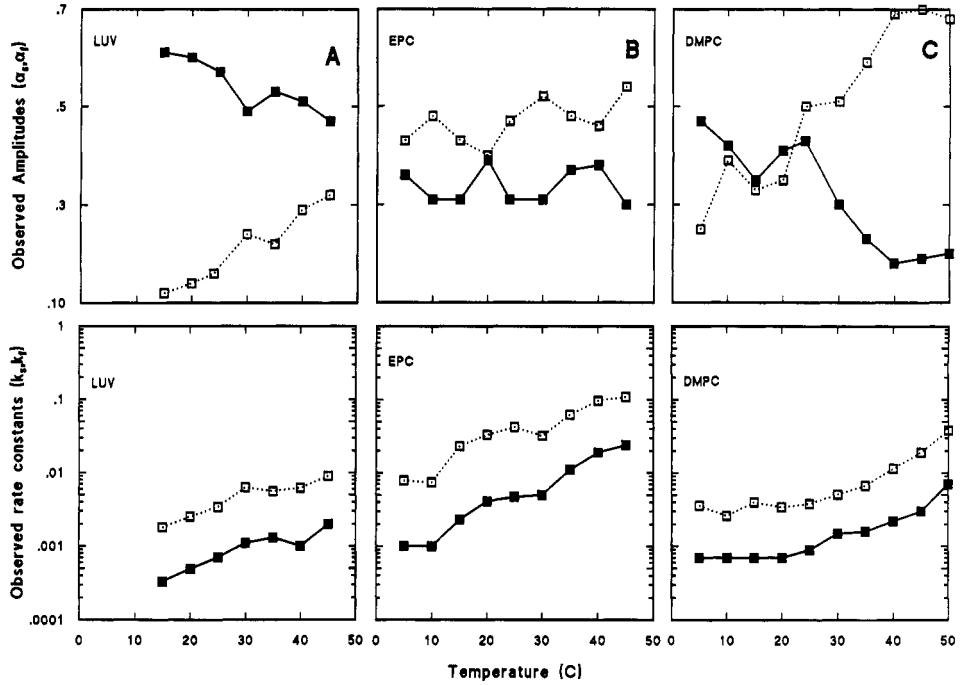

FIGURE 3: Temperature dependence of the observed kinetic parameters. Observed amplitudes (α_s, α_f) and rate constants (k_s, k_f) were obtained by fitting eq 2 to decays (as in Figures 1 and 2, for example) measured at temperatures between 5 and 50 °C. Slow amplitudes and rate constants are represented by solid boxes, and fast parameters are represented by open boxes. Upper and lower panels are values for (A) EPC-LUV, (B) EPC-SUV, and (C) DMPC-SUV.

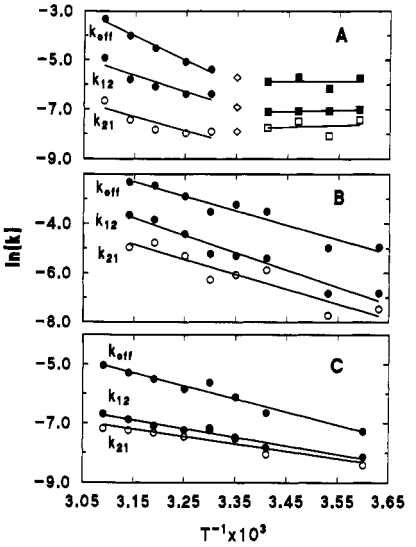

FIGURE 4: Eyring rate analysis of the intrinsic rate constants. Intrinsic rate constants were determined from the observed kinetic parameters using the methods described in the text. The natural logarithm of these values is plotted as a function of the inverse of the absolute temperature. Circles represent values of k_{off} and k_{12} (solid) and k_{21} (open) in the liquid crystalline state, squares represent the corresponding values in the gel state, and the open diamonds represent values for DMPC at 24 °C. Parameters of the solid lines, which are linear fits through all the EPC data and to regions above and below 24 °C for DMPC, were used to determine the activation thermodynamic potentials by Eyring rate theory (Eisenberg & Crothers, 1979). Thus $\Delta H^{*\circ} = -R[T + \mathrm{d}(\ln k)/\mathrm{d}(1/T)]$, $T\Delta S^{*\circ} = RT\ln(k) + \Delta H^{*\circ} - \ln(k_B T/h)$, and $\Delta G^{*\circ} = \Delta H^{*\circ} - T\Delta S^{*\circ}$, where the values of the rate constants at 24 or 25 °C were used, R is the ideal gas constant, k_B is Boltzmann's constant, h is Planck's constant, and $\ln(k_B T/h) = 29.5$ kcal/mol. Values of the activation potentials determined from these results are listed in Table IV.

Table IV: Eyring Rate Theory Analysis of Figure 4 Data[a]

rate constants	$\Delta H^{*\circ}$ (kcal/mol)	$-T\Delta S^{*\circ}$ (kcal/mol)	$\Delta G^{*\circ}$ (kcal/mol)
	EPC-LUV		
k_{12}	5.2	16.8	22.0
k_{21}	4.4	17.7	22.1
k_{off}	8.3	13.0	21.2
	EPC-SUV		
k_{12}	13.5	7.3	20.8
k_{21}	11.5	9.7	21.2
k_{off}	11.1	8.4	19.5
	DMPC-SUV ($T > T_m$)		
k_{12}	12.5	9.3	21.8
k_{21}	10.8	11.3	22.1
k_{off}	18.9	2.1	21.0
	DMPC-SUV ($T < T_m$)		
k_{12}	−1.4	23.1	21.7
k_{21}	−1.3	24.0	22.6
k_{off}	−0.2	21.5	21.2

[a] Methods are as described in the legend to Table I. $\Delta G^{*\circ}$ and $-T\Delta S^{*\circ}$ values were determined at 25 °C for EPC and extrapolated either above or below T_m to 24 °C for DMPC. Uncertainties in these values were estimated to be 0.2 kcal/mol, by standard error propagation methods using uncertainties in the intrinsic rate constants of 30%.

(Wimley & Thompson, 1990). In contrast to these similar trends in off rate behavior, DMPC flip-flop rate constants were much *greater* in LUV than SUV (Wimley & Thompson, 1990), opposite the current results with 12AS. This difference may reflect vesicle composition, since the present comparison of SUV and LUV was done using EPC vesicles, or more likely, it reflects quite different interactions of 12AS versus DMPC with vesicle lipids.

The LUV bilayer more closely reflects the lipid phase of biological membranes than the SUV bilayer. These results, therefore, suggest that the rate of flip-flop of the long-chain AOFA through the lipid phase of biological membranes should be quite slow. Studies of AOFA transport in adipocytes using quantitative fluorescence microscopy do in fact confirm this prediction (Storch et al., 1991). Moreover, the finding that these very hydrophobic molecules ($K_p > 10^5$; Pjura et al., 1984) undergo extremely slow flip-flop directly contradicts the view that lipid bilayer permeability increases with increasing hydrophobicity (Gutknecht & Walter, 1981; Stein,

1986). Specifically, transfer of the much less hydrophobic short-chain AOFA (≤12 carbons) between lipid vesicles proceeds much more rapidly (>100-fold) than the long-chain AOFA (Storch & Kleinfeld, 1986). Since flip-flop is rate-limiting for the long-chain AOFA, this indicates that rates of flip-flop are much slower for long-chain than for short-chain AOFA.

A solution for the kinetic model is essential to interpret correctly the observed decay parameters in terms of the intrinsic rate constants. Although the observed fast rate and the intrinsic off rate constants are approximately equal in the present case of slow flip-flop followed by a faster off step, the flip-flop rates are less directly related to k_s. Four parameters, namely, α_s, k_s, α_f, and k_f (only three are independent since $\alpha_s + \alpha_f + c = 1$), are determined from the observed biexponential decay. Each of these parameters is a specific function of the three intrinsic rate constants k_{12}, k_{21}, and k_{off}; the explicit forms of these functions are the solutions of the kinetic model (Storch & Kleinfeld, 1986; Kleinfeld, 1990). In general, the determination of the intrinsic rate constants and a correct interpretation of the transfer mechanism requires the use of the explicit kinetic model solutions and the complete set of observed kinetic parameters. For example, the *two* observed rate constants (k_s and k_f) are clearly insufficient to determine the *three* intrinsic rate constants. As described in the Materials and Methods, the additional required information is obtained from the observed amplitudes. In addition, the model solution shows that a decay can be well described by a single exponential even when flip-flop and off rates are very different. For example, when $k_{12} \sim k_{off}$, the amplitude of the fast component will be ≤0.05 and therefore transfer kinetics will not be distinguishable from that of a single-exponential decay. Even when flip-flop is much faster than the off step and the kinetics are well described by a single rate constant, the observed single rate constant will not, in general, be equal to the off rate. For example, when $k_{12} = k_{21}$ and in the limit of $k_{12} \gg k_{off}$, the observed rate constant will be equal to $k_{off}/2$ (Kleinfeld, 1990).

Thermodynamics of the Kinetic Barriers. The present results indicate that long-chain AOFA flip-flop and off rates are sensitive functions of vesicle radius of curvature, lipid physical state, and lipid composition. This sensitivity is reflected in the variation of enthalpic and entropic contributions to the free energy of 12AS transfer in the different vesicle systems (Table IV). These energies reflect the underlying molecular interactions between 12AS and the lipid host. Although a detailed molecular model of AOFA movement is premature, it is likely that in order to leave the bilayer or to transfer from one hemileaflet to the other, interactions between 12AS and the host lipid and interfacial regions must be momentarily relaxed. We envision, in much the same way as discussed by Wimley and Thompson (1991), that the transition state for flip-flop involves the formation of a transitory hole or defect within one hemileaflet of the bilayer and relaxation of 12AS–phospholipid interactions in the other. This latter process, together with the formation of a hole in the water–lipid interfacial region, is probably required for the off step as well. The transition state for the off step itself is probably one in which the carboxyl group and part of the acyl chain is hydrated, while the terminal portion of the chain remains associated with the membrane lipids (Doody et al., 1980; McLean & Phillips, 1984b).

DMPC-SUV < T_m. The most dramatic differences in the thermodynamic characteristics among the vesicle systems is exhibited by gel-state DMPC-SUV. Both the off step and flip-flop of 12AS have essentially zero enthalpy, and therefore, the barriers for 12AS desorption and flip-flop are almost entirely entropic in the DMPC gel state (Table IV). For the off step, the entropic barrier could result from a final state of lower entropy than the initial state and/or from a low-entropy transition state. Two interactions probably contribute to reducing the final and/or transition state entropy: (1) 12AS interacting with water reduces entropy because of the hydrophobic effect (Tanford, 1973) and (2) the order of the gel-state bilayer increases once the perturbing 12AS is removed, thereby allowing those DMPC molecules previously in contact with 12AS to return to the gel state. These negative entropy contributions will be offset to some extent by the approximately −10 kcal/mol ($-T\Delta S$) resulting from the increase in the translational and rotation motion upon FA transfer from the two-dimensional bilayer to the three-dimensional aqueous phase (McLean & Phillips, 1981). However, because the entropic barriers for 12AS desorption from DMPC < T_m is 21 kcal/mol (Table IV) and the entropic contribution ($-T\Delta S$) of the hydrophobic effect is probably less than about 10 kcal/mol (Tanford, 1973), a negative entropy contribution from the bilayer very likely contributes to the off step. Thus removal of 12AS, with its bulky anthroyloxy group, from the gel-state DMPC bilayer probably results in the increased order reflected in the negative entropy barrier. The barrier for flip-flop, which is also virtually all entropic, probably involves similar events as for desorption. The flip-flop barrier most likely involves the formation of a low-entropy *transition* state, since, to a first approximation, the initial (AOFA in one hemileaflet of the bilayer) and final (AOFA in the other hemileaflet of the bilayer) states in the gel-phase SUV are similar.

The zero enthalpy for desorption of 12AS from gel-state DMPC-SUV (Table IV) represents the limit of similar trends reported for the short-chain FA 9-(3-pyrenyl)nonanoic acid (Doody et al., 1980) and for DMPC (McLean & Phillips, 1984b). In these previous studies, the enthalpy change for the off step was found to be smaller and the entropy differences were more negative below than above the phase transition temperature of DMPC-SUV. In contrast, the DMPC off step from DMPC-LUV was found to be a predominantly enthalpic process with a small but *positive* entropy change (Wimley & Thompson, 1990). Wimley and Thompson (1990) suggested that these differences in DMPC desorption result from a more ordered LUV than SUV gel state. As a consequence of this more ordered state, DMPC–DMPC enthalpic interactions are presumably greater in LUV than SUV. Quite the opposite would be expected for 12AS, whose perturbing structure would be expected to both reduce DMPC–DMPC interactions and have much smaller enthalpic interactions with DMPC. This is likely the case in SUV, and we would predict even greater entropic barriers for 12AS desorption in gel-state LUV.

LUV. Kinetic barriers for LUV are also dominated by entropic factors, suggesting similar interactions as in DMPC-SUV below T_m. Not surprisingly, the entropy changes in the liquid crystalline phase LUV are smaller than for the DMPC gel state. Although introduction of 12AS into the liquid crystalline phase of the bilayer disorders lipid acyl chains, this is likely to be a smaller perturbation than in the gel state, and thus the release of this perturbation will have a correspondingly smaller effect on the reduction of entropy. Unlike the DMPC gel state, however, enthalpic contributions are significant in both the AOFA flip-flop and the off steps in LUV. If formation of the transition states involves the creation

of similar defects as for the gel-state DMPC, where enthalpic contributions are negligible, then the difference between SUV $< T_m$ and LUV suggests that the enthalpic interactions between 12AS and lipid must be sensitive to the phospholipid phase. Greater acyl chain flexibility in the liquid crystalline phase may allow the formation of favorable 12AS–phospholipid interactions which are sterically prevented in the gel phase. Formation of the LUV transition state would then involve breaking of 12AS–phospholipid interactions. Significant enthalpic contributions to the 12AS–lipid interactions are consistent with the "nonclassical hydrophobic effect" recently described by Seelig and Ganz (1991). In these studies enthalpic interactions, probably arising from van der Waals interactions between the amphiphiles and the hydrophobic lipid core, were found to dominate ($\Delta H \sim -9$ kcal/mol) the equilibrium binding of a variety of amphiphiles to liquid crystalline phase lipid bilayers, and we suggest that similar interactions occur between 12AS and the hydrophobic lipid core.

SUV > T_m. Entropic contributions to all three kinetic barriers are considerably smaller in liquid crystalline phase SUV than in LUV (Table IV). For flip-flop, these barriers probably reflect lower transition-state entropies in SUV than in LUV, since to a first approximation initial and final (ground) states in both types of vesicles are similar. Moreover, it is unlikely that the 12AS-LUV ground state is more disordered than the 12AS-SUV ground state since lipid order differences in liquid crystalline phase LUV and SUV are relatively small and in fact favor slightly more ordered phospholipid acyl chains in LUV (Lepore et al., 1992). Thus the defect or hole formed by the transition state in SUV is probably more disordered than in LUV, analogous to the mechanism suggested for DMPC flip-flop in gel-phase vesicles and in DMPC/DMPE LUV (Wimley & Thompson, 1990, 1991).

For the off step as well, the entropic barriers are probably due to increased order of the transition state as compared to the ground states. As discussed above for LUV, the entropic barrier for the off step from SUV probably results from the formation of an ordered transition hole or defect. This view is also supported by the finding of low equilibrium entropy differences for transfer of amphiphiles from water to bilayers (Seelig & Ganz, 1991), and therefore only the transition state should contribute significantly to the entropic contribution to the off step. Moreover, for the reasons given above for flip-flop and because there is probably little difference in ground-state entropies, the greater entropic barrier for LUV likely reflects the formation of more ordered defects in the off step transition state. The results for 12AS transfer in gel-state DMPC-SUV suggest that enthalpic interactions with water should not contribute significant positive free energy to the transition state. The large enthalpic contributions found for the off step and flip-flop above the T_m suggest that van der Waals interactions between 12AS and phospholipids occur either in the ground or transition state, when phospholipids can assume the requisite conformations relative to the 12AS surface. That these interactions are greater in SUV than in LUV is consistent with the more disordered defect suggested for the SUV transition state.

Larger $\Delta G^{\ddagger\circ}$ values for DMPC as compared to EPC may reflect the greater saturation of DMPC acyl chains. As seen in Table IV, the entropic components represent the largest contributions to the $\Delta G^{\ddagger\circ}$ differences between DMPC and EPC. Thus, even in the liquid crystalline phase, formation of the transition state in DMPC may lead to a greater degree of order than in EPC. The origin of the very small entropic and correspondingly large enthalpic contributions to the off step in DMPC is unclear. It is possible, since SUV exhibit a broad phase transition, that they are partially gel phase at temperatures above 24 °C, resulting in smaller k_{off} values than would occur if the vesicle were uniformly liquid crystalline.

These studies were done to better understand the mechanism of membrane transfer of fatty acids and amphiphiles in general. Given the very different behavior of 12AS and DMPC in LUV (Wimley & Thompson, 1990), it is difficult to extrapolate the present results for FA analogs to amphiphiles in general. Nevertheless, the present 12AS results do bear considerable similarities to results obtained with cholesterol, pyrenyl FA, and even DMPC in SUV. The observed decrease (~10-fold) in transfer rate of 12AS between LUV as compared to SUV is similar to the decrease (~5-fold) observed for cholesterol transfer between larger as compared to smaller vesicles (McLean & Phillips, 1984a). The *decrease* in 12AS activation enthalpy below as compared to above T_m for DMPC-SUV ($\Delta\Delta H^{\ddagger\circ} = 19$ kcal/mol), although greater in magnitude, is the same direction trend observed for the transfer of 9-(3-pyrenyl)nonanoic acid (Doody et al., 1980) ($\Delta\Delta H^{\ddagger\circ} = 3.7$ kcal/mol) and DMPC (McLean & Phillips, 1981) ($\Delta\Delta H^{\ddagger\circ} = 8.6$ kcal/mol). These similarities among several quite different amphiphiles suggest that while the magnitudes of the kinetic barriers are sensitive to amphiphile structure, the molecular interactions that determine the barriers may be similar.

Thus, if transfer occurs by a similar mechanism as for 12AS, the present studies raise the possibility that natural long-chain FA will exhibit rates of flip-flop across lipid bilayers that are too slow to achieve physiologically required transport rates. In this event, cellular transport of the physiologically important FA could require the action of a membrane protein to overcome the lipid barrier to membrane permeability. The results of our adipocyte studies, indicating membrane protein mediated transport of long-chain AOFA, do in fact demonstrate competitive inhibition by unlabeled oleic acid, suggesting that the unlabeled FA are the natural substrates for this transporter (Storch et al., 1991). Nevertheless, as discussed in the introduction, there is considerable controversy associated with the problem of unlabeled FA movement across membranes. This controversy is a consequence of the inability to measure movement of aqueous-phase monomers of long-chain unlabeled FA from one side of a membrane to the other, directly and with sufficient temporal resolution. Recently, a fluorescent probe has been developed that should allow such measurements (Richieri et al., 1992). Preliminary results using this probe to measure oleate movement across red cell ghosts indicate that long-chain FA transport is protein-mediated (Kleinfeld & Chu, 1993).

REFERENCES

Abumrad, N. A., Park, J. H., & Park, C. R. (1984) *J. Biol. Chem. 259*, 8945–8953.

Cardoza, J. D., Kleinfeld, A. M., Stallcup, K. C., & Mescher, M. F. (1984) *Biochemistry 23*, 4401–4409.

Cooper, R. B., Noy, N., & Zakim, D. (1989) *J. Lipid Res. 30*, 1719–1726.

Daniels, C., Noy, N., & Zakim, D. (1985) *Biochemistry 24*, 3286–3292.

DeGrella, R. F., & Light, R. J. (1980) *J. Biol. Chem. 255*, 9739–9745.

Doody, M. C., Pownall, H. J., Kao, Y. J., & Smith, L. C. (1980) *Biochemistry 19*, 108–116.

Eisenberg, D., & Crothers, D. (1979) *Physical chemistry with applications to the life sciences*, 1st ed., The Benjamin/Cummings Publishing Company, Inc., Menlo Park, CA.

Gutknecht, J. (1988) *J. Membr. Biol. 106*, 83–93.
Gutknecht, J., & Walter, A. (1981) *Biochim. Biophys. Acta 645*, 161–162.
Hamilton, J. A. (1989) *Proc. Natl. Acad. Sci. U.S.A. 86*, 2663–2667.
Huang, C., & Thompson, T. E. (1974) *Methods Enzymol. 32*, 485–489.
Kleinfeld, A. M. (1990) *Comments Mol. Cell. Biophys. 6*, 361–383.
Kleinfeld, A. M., & Chu, P. (1993) *Biophys. J.* abstracts (in press).
Lepore, L. S., Ellena, J. F., & Cafiso, D. S. (1992) *Biophys. J. 61*, 767–775.
McLean, L. R., & Phillips, M. C. (1981) *Biochemistry 20*, 2900–2908.
McLean, L. R., & Phillips, M. C. (1984a) *Biochim. Biophys. Acta 776*, 21–26.
McLean, L. R., & Phillips, M. C. (1984b) *Biochemistry 23*, 4624–4630.
Morand, O., & Aigrot, S. (1985) *Biochim. Biophys. Acta 835*, 68–76.
Noy, N., Donnelly, T. M., & Zakim, D. (1986) *Biochemistry 25*, 2013–2021.
Nozaki, Y., Lasic, D. D., Tanford, C., & Reynolds, J. A. (1982) *Science 217*, 366–367.
Nunn, W. D., Simons, R. W., Egan, P. A., & Maloy, S. R. (1979) *J. Biol. Chem. 254*, 9130–9134.
Paris, S., Samuel, D., Romey, G., & Ailhaud, G. (1979) *Biochimie 61*, 361–367.
Pjura, W. J., Kleinfeld, A. M., & Karnovsky, M. J. (1984) *Biochemistry 23*, 2039–2043.
Potter, B. J., Sorrentino, D., & Berk, P. D. (1989) *Annu. Rev. Nutr. 9*, 253–270.
Richieri, G. V., Ogata, R. T., & Kleinfeld, A. M. (1992) *J. Biol. Chem. 267*, 23495–23501.
Seelig, J., & Ganz, P. (1991) *Biochemistry 30*, 9354–9359.
Shohet, S. B., Nathan, D. C., & Karnovsky, M. L. (1968) *J. Clin. Invest. 47*, 1096–1108.
Stein, W. D. (1986) *Transport and diffusion across cell membranes*, Academic Press, Inc., Orlando, FL.
Storch, J. (1990) *Hepatology 12*, 1447–1449.
Storch, J., & Kleinfeld, A. M. (1986) *Biochemistry 25*, 1717–1726.
Storch, J., Lechene, C., & Kleinfeld, A. M. (1991) *J. Biol. Chem. 266*, 13473–13476.
Tanford, C. (1973) *The Hydrophobic Effect: Formation of Micelles and Biological Membranes*, John Wiley and Sons, New York.
Wimley, W. C., & Thompson, T. E. (1990) *Biochemistry 29*, 1296–1303.
Wimley, W. C., & Thompson, T. E. (1991) *Biochemistry 30*, 1702–1709.